

Chapter 3- Experimental



In the present study, bismuth ferrite and gadolinium doped bismuth ferrite have been synthesized. Reduced graphene oxide (rGO) and nitrogen doped reduced graphene oxide (N-rGO) are also prepared as a carbonaceous support. Further, heterojunctions have been synthesized between bismuth ferrite and Gd doped bismuth ferrite with the supports.

### **3.1 Synthesis of supports**

#### **3.1.1 Graphite oxide (GO)**

Graphite powder was used to prepare GO as per Hummer's method [199]. Graphite powder (3.0 g) and sodium nitrate (1.5 g) were added into 150 mL concentrated H<sub>2</sub>SO<sub>4</sub>. Then, potassium permanganate (12 g) was added slowly to the reaction mixture with constant stirring and 20°C. The mixture was kept for incubation at 35 °C for 120 min using a hot plate. Double distilled water (150 mL) was added tardily to avoid a quick increase in temperature due to the exothermic reaction. The reaction was ended by the addition of double-distilled water (250 mL), and 60 mL 30% hydrogen peroxide aqueous solution was also added to the mixture to dissolve permanganate residue. The solid product was obtained by centrifugation (3000 r min<sup>-1</sup>) and was washed with 10% HCl solution repeatedly until residual salts were removed. The solid product was dried at 70<sup>0</sup> C in the oven to obtained GO (~5 g).

#### **3.1.2 Reduced graphene oxide (rGO)**

GO was reduced by hydrothermal dehydration method as described by Zhou et al. [200]. In contrast to other methods, supercritical water was used instead of other organic solvent and harmful reducing agent, which offers green chemistry. For reduction, the prepared GO was dispersed into deionized water and the solution (5 mg. mL<sup>-1</sup>) was treated hydrothermally in a Teflon-lined stainless-steel autoclave (150 mL) at 200<sup>0</sup> C for 8 h. Subsequently, the solid product was rinsed with double distilled water followed by

methanol repeatedly. Reduced graphene oxide (rGO, ~500 mg) was obtained after keeping dry at 60 °C overnight.

### **3.1.3 Nitrogen-doped graphene oxide (N-rGO)**

Graphite flakes (3.0 g), NaNO<sub>3</sub> (1.5 g) and H<sub>2</sub>SO<sub>4</sub> (150 mL) were mixed at 15 °C. KMnO<sub>4</sub> (12 g) was added gradually into the solution. Then, melamine (1.5 g) was added to the solution and was stirred constantly for 12 h at 35 °C [201]. N-GO was obtained by following the same method as described in the preparation of GO. Nitrogen-doped reduced graphene oxide (N-rGO, 10% nitrogen doping) was obtained by the hydrothermal process, as described in the preparation of reduced graphene oxide.

## **3.2 Synthesis of photocatalysts**

### **3.2.1 Bismuth ferrite (BFO)**

BFO was prepared by adding 7.6 g of bismuth nitrate (Bi (NO<sub>3</sub>)<sub>3</sub>·5H<sub>2</sub>O) to 100 mL ethylene glycol (EG). The mixture was kept for sonication at room temperature (~25<sup>0</sup> C) for 15 min to form a solution. Ferric nitrate (Fe (NO<sub>3</sub>)<sub>3</sub>·9H<sub>2</sub>O) was then added to the solution in a stoichiometric ratio and kept for sonication at room temperature until a brownish-red solution was obtained. The solution was kept at 70<sup>0</sup> C for 20 h to form a xerogel. After calcination of xerogel in a muffle furnace at 600<sup>0</sup> C for 3 h, bismuth ferrite (~9 g) powder was obtained [202].

### **3.2.2 Gadolinium doped bismuth ferrite (BGFO)**

A stoichiometrically equivalent amount of Bi (NO<sub>3</sub>)<sub>3</sub>·5H<sub>2</sub>O (7.6 g) and Gd (NO<sub>3</sub>)<sub>3</sub>·6H<sub>2</sub>O (1.38 g) were mixed, dissolved in acetic acid (C<sub>2</sub>H<sub>4</sub>O<sub>2</sub>) and ethylene glycol (C<sub>2</sub>H<sub>6</sub>O<sub>2</sub>), and stirred for 90 min at room temperature. Fe (NO<sub>3</sub>)<sub>3</sub>·9H<sub>2</sub>O (6.1 g) powders were dissolved in acetic acid with constant magnetic stirring for 1.5 h and again made a solution of Fe (NO<sub>3</sub>)<sub>3</sub>·9H<sub>2</sub>O on dissolving in acetic acid. After this, both the solutions were mixed and set to a constant stirring for 3 h. Excess bismuth ferrite (3% wt/wt) was

used to compensate for the bismuth loss during the heating process. The as-prepared solution was dried in an oven at 80 °C for 12 h to get a gel and then calcined in a furnace at 600 °C for 3 h [203]. Gd-doped bismuth ferrite (~10 g, stoichiometrically 10% Gd) powder was obtained.

### **3.3 Synthesis of heterojunctions**

#### **3.3.1 rGO supported bismuth ferrite (BFO/rGO)**

For the preparation of BFO/rGO, 200 mg of each rGO was dispersed with 2 g BFO into an aqueous solution (DMF: water:: 1:2) and kept stirring for 2 h to form a stable suspension. After stirring for 2h at room temperature, the solution was treated hydrothermally in a Teflon-lined stainless-steel autoclave at 200<sup>0</sup> C for 15 h. Subsequently, the solid product was rinsed with double distilled water and methanol repeatedly and dried at 70<sup>0</sup> C.

#### **3.3.2 N-rGO supported bismuth ferrite (BFO/N-rGO)**

For the preparation of BFO/N-rGO, 200 mg of each rGO was dispersed with 2 g BFO into an aqueous solution (DMF: water:: 1:2) and treated it hydrothermally by following exact same procedure as described in the synthesis of BFO/rGO (section 3.3.1).

#### **3.3.3 N-rGO supported Gd-doped bismuth ferrite (BGFO/N-rGO)**

For the preparation of BGFO/N-rGO composite, 200 mg of N-rGO was dispersed with 2g BFO into an aqueous solution (DMF: water:: 1:2) and kept stirring for 2 h to form a stable suspension. After stirring for 2h at room temperature, the solution was treated hydrothermally in a Teflon-lined stainless-steel autoclave (150 mL) at 200<sup>0</sup> C for 15 h, and the autoclave was cooled at room temperature. Subsequently, the solid product was rinsed double distilled water and methanol repeatedly and finally dried at 70<sup>0</sup> C in the oven.

### 3.4 Experimental Setup and activity measurements

Photocatalytic and sono-photocatalytic degradation of Rhodamine B (RhB) were carried out in a cylindrical quartz reactor (length -30 cm, diameter- 5 cm). The reactor had two outlets; one was used for gas exit and a second outlet for sample collection. Hg arc lamp was used as a source of light. The experimental setup is shown in Fig. 3.1. Its diagrammatic representations are shown in Fig. 3.2 (a and b) that are used in photocatalytic and sono-photocatalytic degradation of RhB, respectively. A PZT transducer type ultrasonic generator was used to produce 20 kHz frequency at various power inputs.

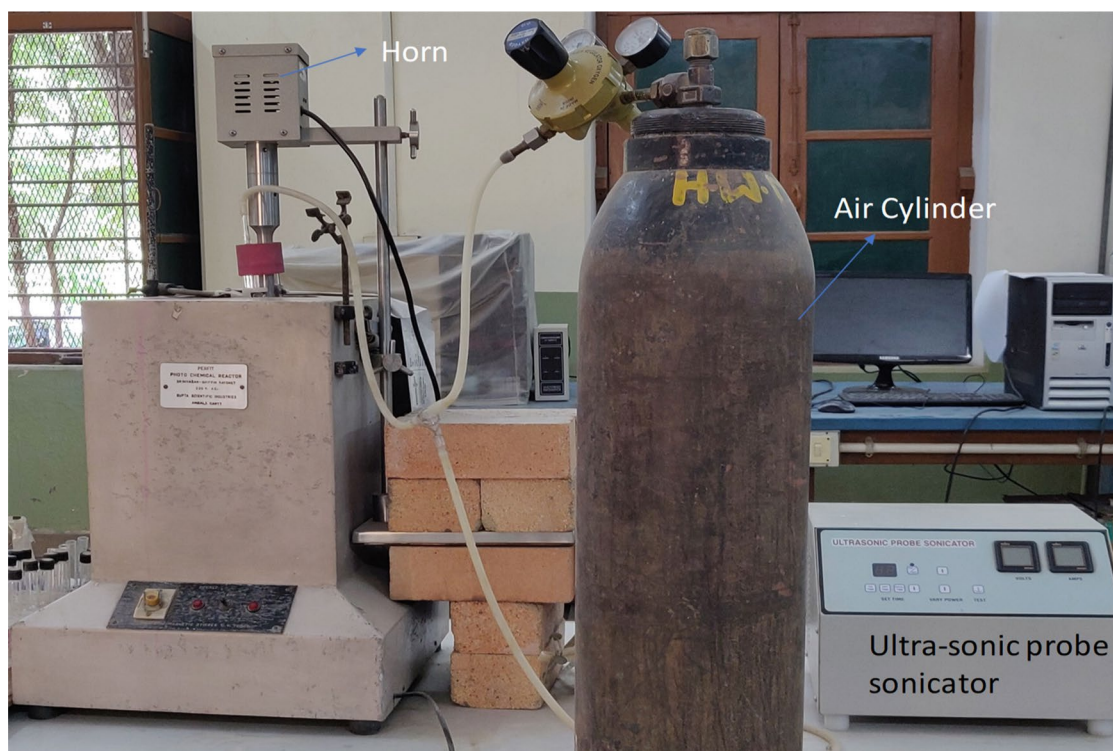


*Fig. 3. 1 Experimental setup.*

A stock solution of RhB (100 mg/L) was prepared. Then, an aqueous solution of RhB (250 ml) containing a certain amount of catalyst and with an initial concentration of 10 mg. L<sup>-1</sup> was poured into 300 mL quartz cylindrical reactor. Before switching on the light source, the solution was agitated in the dark for 120 min by passing N<sub>2</sub> gas to achieve equilibrium (adsorption-desorption) between photocatalyst and RhB. Air was used for

the oxidation process by passing into the solution. After switching on the light, the sample was collected after every 30 min of reaction. UV-Vis spectrophotometer was used to

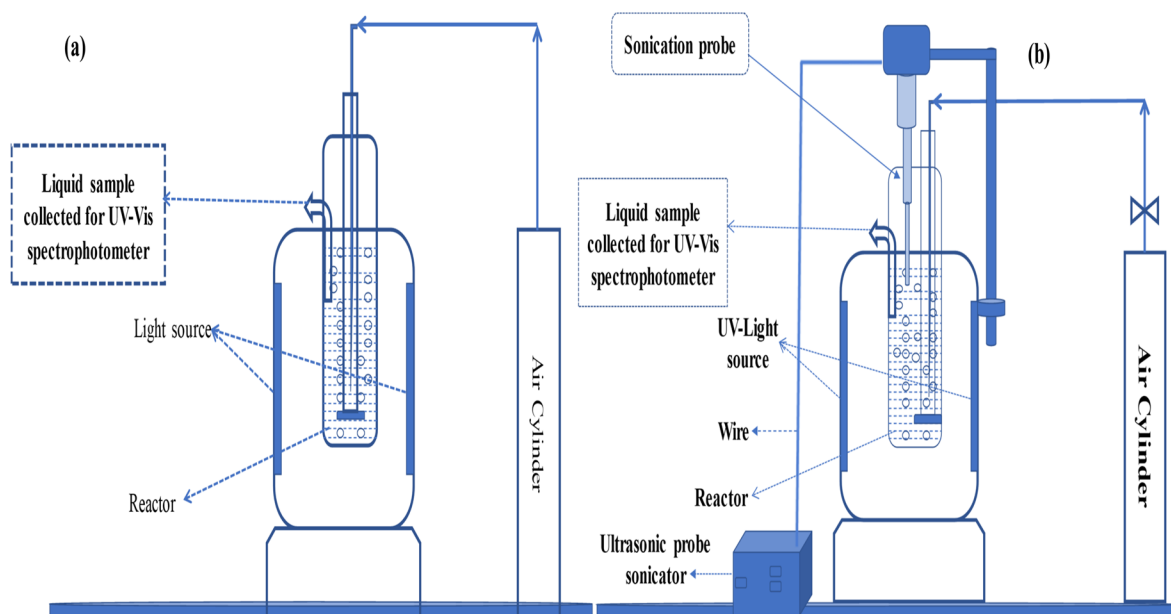


Fig. 3. 2 A diagrammatic representation of (a) Photocatalytic process; (b) Sono-photocatalytic process.

compute the concentration of RhB at maximum wavelength 553 nm on the basis of Lambert-Beer's law.

Several scavengers viz, 1-4 benzoquinone (1-4 BQ), tert-butyl alcohol (TBA), potassium dichromate (PD) and ammonium oxalate (AO) for  $O_2^-$ ,  $OH^\cdot$ ,  $e^-$  and  $h^+$  respectively, were used for the identification of reactive species [260-264]. These scavengers were added separately or in combination to the reaction mixture and were measured after a fixed interval of 30 minutes as described above.

### 3.5 Contamination source: Rhodamine B

Use of a high amount of organic dye is most common in the textile industry; therefore, some amount remains in the effluent. At global level, more than  $7 \times 10^5$  tons of 100,000 different types of dyes are being produced annually, and most of them are very difficult to decompose due to their complex structure. Different types of dyes include acidic, basic,

azo, diazo, metal complex dyes, etc. These dyes remain untreated in aerobic methods of the municipal sewerage systems [79]. Among different dyes, xanthenes are the second highest-studied group of dyes dominated by rhodamine B.

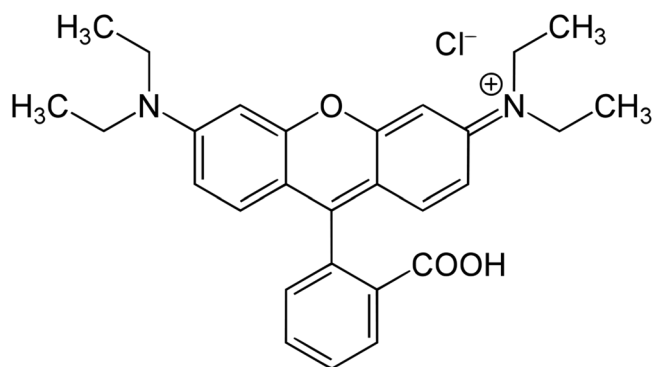


*Fig. 3. 3 Chemical structure of rhodamine B.*

Rhodamine B (abbreviation: RhB; C.I. Basic Violet 10; C.I. number: 45170; chemical class: xanthene; molecular formula:  $C_{28}H_{31}N_2O_3Cl$ ). Rhodamine B (molecular weight:  $479.01 \text{ g mol}^{-1}$ ); IUPAC Name N-[9-(ortho-carboxyphenyl)-6-(diethylamino)-3H-xanthen-3-ylidene] diethyl ammonium chloride, which is highly water-soluble, was used as a model solute in the present study. The molecular structure of RhB is shown in Fig. 3.3.

### 3.6 Materials

Graphite powder from Aldrich was used for preparation of support GO and doped GO. Sodium nitrate, sulfuric acid, potassium permanganate, and hydrochloric acid were of reagent grade.  $H_2O_2$  (30% W/V) was used from Rankem Limited. Bismuth nitrate, ferric nitrate, gadolinium nitrate, ethylene glycol, and acetic acid were from Siga-Aldrich.

### 3.7 Characterization of tools

Characterization of catalysts is the predominant part of catalytic research. Knowledge of the characterization process can help to understand the relationship between catalyst



behaviour and catalyst composition and structure. While many characterization methods can provide valuable results on catalytic properties, the most useful and meaningful information almost always comes from a combination of characterization methods. Following characterization techniques were used to study microstructure of supports and catalysts, and to develop interrelation between the photoactivity, microstructure of the catalysts and their preparation techniques. Characterization techniques used in the present study are reported in the Table 3. 1.

*Table 3. 1 Instruments used in the present study.*

<b>S. No.</b>	<b>Instrument</b>	<b>Uses</b>
1	X-Ray diffraction (XRD)	Crystal structure- phase identification and crystallite size
2	Fourier transform infrared spectroscopy (FTIR)	Functional group analysis
3	Diffuse reflectance spectroscopy (DRS)	UV and Visible light absorption and band gap estimation of the catalysts
4	Photoluminescence spectroscopy (PL)	Charges recombination study
5	Scanning electron microscope (SEM)	Morphological study
6	Energy Dispersive X-ray Analysis (EDX)	Surface elemental analysis
7	Transmission electron microscope (TEM)	Imaging and particle size

8	Selected area diffraction pattern (SAED)	Crystal structure
9	X-ray photoelectron spectroscopy (XPS)	Surface analysis, and to examine the element composition
10	Electrochemical impedance spectroscopy (EIS)	Study of charge transfer resistance and conductivity
12	Mott. Schottky analysis	Carrier concentration, Flat band potential
13	BET surface area	Surface area analysis

### 3.7.1 X-ray diffraction (XRD)

X-ray diffraction technique is used to study the structural information of materials. In this technique, the incident X-rays interacts with the specimen and diffracts. Finally, diffracted patterns are collected as a result of constructive interference according to the Braggs Law:

$$n\lambda = 2d_{hkl} \sin\theta \quad (3.1)$$

Where, n is the order of reflection (any value integer), 1 to be taken for first-order reflection,  $\lambda$  = wavelength of the incident, X-rays  $d_{hkl}$  = interplanar spacing and  $\theta$ = Braggs diffraction angle. Crystallite sizes (L) were calculated by using Scherrer equation (Eq. 3.2)

$$L = \left( \frac{K\lambda}{\beta \cdot \cos\theta} \right) \quad (3.2)$$

Where, K= Scherrer constant (in the present study 0.9 to be taken for spherical particle),  $\beta$  = Full width at half of the maximum (FWHM) of a reflection peak after subtracting contribution due to the instrumental broadening.

In the present study, X- ray diffraction patterns of the prepared catalysts were obtained from a Rigaku Ultima IV diffractometer using Cu – K $\alpha$  irradiation of wavelength 1.542 Å. The calculated d-values were matched with standard data for identification of different phases present in various catalysts. The mean crystallite sizes (L) of the catalysts were calculated by measuring the line broadening and using the Scherrer formula written above (Eq. 3.2). Generally, there are the three sources which consider for peak broadening as given below

- (a) Instrumental contribution
- (b) Sample contribution
- (c) Strain contribution

Since, catalysts were sulfides, internal strain was neglected. Instrumental broadening needs to be corrected by subtracting from the total broadening ( $\beta_{Total}$ ) by using the following equation.

$$\beta_{Total} = \beta_{instrument}^2 + \beta_{sample}^2 \quad (3.3)$$

The instrumental broadening is obtained from the diffraction pattern of a “standard sample” which consists of large crystallites. In our sample standard sample was ‘Si’, and broadening ( $\beta_{instrument}$ ) was 0.079.

### **3.7.2 Fourier transform infrared spectroscopy (FTIR)**

In current study, a Nicolet 5700 (Thermo Electron) FTIR spectrophotometer was used to record FTIR spectra in mid IR range (4000–600 cm<sup>-1</sup>). An average of 16 spectra in diffuse reflectance mode was recorded at room temperature at the resolution of 8 cm<sup>-1</sup>. KBr was used as a reference material. About 1 mg of the sample and 100 mg of KBr were well ground with the help of pastel and mortar.

### 3.7.3 Diffuse reflectance spectroscopy (DRS)

It is an effective spectroscopic tool to estimate the band gap of semiconductor photocatalyst and the light absorption characteristics of catalysts. When the powdered sample is radiated with light, a portion of radiation is reflected at a powder surface and the remaining are either absorbed or transmitted by the powder. With an integrating sphere attached to the UV-Vis spectrophotometer (Diffuse reflectance spectroscopy) it is possible to again direct the reflected light to fall on the sample are obtained.

In the present study, diffuse reflectance spectroscopy of catalysts was carried out on UV-Vis spectrophotometer (Varian 100Bio) with a total reflection attachment. BaSO<sub>4</sub> was used as a reflectance standard. Absorbance data were used for the Tauc plot using the Kubelka-Munk transformation as given by the equation:

$$(\alpha h\nu)^n = A (h\nu - E_g) \quad (3.4)$$

Where,  $h$  is the Planck constant,  $\nu$  is the frequency of the light source,  $\alpha$  is absorption coefficient,  $A$  is a proportional constant,  $E_g$  is the band gap, and  $n$  signifies the nature of the electron transition. For direct transition (in case of BiFeO<sub>3</sub>) a plot of  $(\alpha h\nu)^2$  vs  $h\nu$  will yield a straight line. Intercept of the line on the x-axis gives the band gap.

### 3.7.4 Photoluminescence spectroscopy (PL)

Photoluminescence (PL) spectroscopy is a non-destructive technique. In this technique, first photo excitation process is executed by absorption of the light by a sample. An electron moves to excited state due to photo-excitation, which subsequently comes back to its equilibrium state. During the photo excitation, an electron may jump from the valence band and move to conduction band and subsequently come back to valence band which is called recombination. During this process, excess energy is released through emission of light. This excess energy is equal to the energy difference between the equilibrium and excited states. This emitted light is detected by photon detector through

a spectrometer to give PL spectra. Thus, the emission spectra corresponding to band-gap excitation may yield valuable information about recombination behavior of photocatalysts. Recombination behavior of catalysts was studied to establish its relation with photocatalytic activity and microstructure. In the present study, PL spectra were obtained using Fluorescence Spectrophotometer (Varian, Cary eclipse). Powder samples were placed in a sample holder. Excitation wavelength was 200 nm. Emission wavelengths were recorded from 400 to 600.

### **3.7.5 Scanning electron microscope (SEM)**

An electron microscope is a tool that uses high-energy electron beams to inspect very small level. This audit can provide information about the topography (surface properties) of the sample and the morphology (shape and size) of the sample. Scanning electron microscopy (SEM) scanning develops an image by scanning the sample surface with an electron probe rasterized with a cathode ray tube electron beam (CRT or TV phototube). In this study, the surface morphology of the catalysts is characterized using SEM. The SEM micrographs of the samples were taken using FEI™, Quanta 200F instrument.

### **3.7.6 Energy dispersive X-ray (EDX)**

Energy dispersive method is used to affirm the presence of chemical element on the catalytic surface. Elemental analysis data obtained using EDX can be used to observe the presence of dopant and impurities on the surface of the catalyst. All dopants that were not detected by XRD analysis were observed with EDX. EDX spectra of the samples were recorded in a Model FEI™, Quanta 200F instrument.

### **3.7.7 Transmission electron microscope (TEM) and selected area electron diffraction (SAED)**

Transmission electron microscopy was used to image and analyze the microstructure of the photocatalytic materials. Measurements were performed in a TecnaiG2 20 make TEM

at 200 kV accelerating voltage. Powder samples were homogeneously dispersed in pure ethanol by means of an ultrasonic bath and then deposited on a copper grid and the solvent was allowed to evaporate under vacuum before analysis. Selected area electron diffraction (SAED) uses diffracted electrons to elucidate crystallographic information from selected regions of the sample. This attachment was employed with TEM. The diffraction pattern was of a thin sample recorded simultaneously with TEM. The spacing and orientation of the diffraction spots can be interpreted in terms of planar spacing similar to the XRD.

### **3.7.8 X-ray photoelectron spectroscopy (XPS)**

X-ray photoelectron spectroscopy (XPS) is the prominent tool for detecting elemental identification and its oxidation state on solid surfaces. In this technique, the spectra can be obtained by irradiating a sample with X-rays beam while simultaneously measuring the kinetic energy and number of electrons that escape from sample being analyzed. Ultra-high vacuum (UHV) condition is required during analysis. Soft X-rays targets (i.e. Mg K $\alpha$ ) are used as a source. Photons are absorbed by specimen and then electrons are ejected via the photoelectric effect. The energy of the ejected electrons can be written as:

$$E_{KE} = h\nu - E_{BE} \quad (3.5)$$

Where,  $E_{KE}$  is the kinetic energy of ejected electron,  $h\nu$  is the energy of incident photon and  $E_{BE}$  is the energy of an electron in bound state. Binding energy is specified for individual elements. Therefore, identification of particular element becomes possible by measuring the photoelectron energy. It should be noted that for multi-component samples the intensities of the peaks are proportional to the concentration of the element within the sampled region.

In the present study, XPS studies were carried out on AMICUS, Kratos Analytical using monochromated Mg K $\alpha$  (1253.6 eV) as X-ray source. A vacuum of  $2 \times 10^{-7}$  kPa was

maintained in the analyzer chamber. A value of 284.6 eV for the carbon C 1s peak was used as calibration for all measurements. Raw peaks were de-convoluted accurately using XPS peaks 4.1 software.

### **3.7.9 Electrochemical impedance spectroscopy (EIS)**

Electrical properties of material as well their interface with surface modified electrode can be evaluated by this technique. The response of the electrochemical system is very nonlinear. The resistance of the system is usually displayed in Nyquist plot, with the reactance inverted (since such systems are inherently capacitive). Where, Impedance ( $Z$ ) is a determination of the circuit characteristics to impede the flow of electron when exposed to a periodic electrical perturbation.  $R_s$  is resistance due to solution/electrolyte.  $R_{ct}$  is the resistance associated with an electrode reaction i.e. related to generation of electron and transfer to bulk.  $C_d$  is the capacitance, created due to bulk and interface.

Impedance spectroscopy was done using an Autolab (PGSTAT 204) electrochemical work station with impedance analyzer in a two-electrode configuration. For the electrode fabrication, Toray Carbon Paper (TGP-H-60, Alfa Aesar, USA) having 0.25 cm<sup>2</sup> cross-sectional area was used. Slurry was prepared by dispersing the required quantity of photocatalyst powder in Nafion solution with a few drops of DMF followed by sonication in ultrasonic water bath for 1 h for better dispersion. The slurry was drop cast on the carbon paper. It was then dried in air for 6 h. Before the impedance scanning experiments, the remaining surface was polished to minimize ohmic effect. The electrolyte was a solution of sulphite and sulphide ions which was used for photoelectrochemical activity measurement.

### 3.7.10 Mott-Schottky (M-S)

The Mott-Schottky technique is a powerful tool for the study of electrode surfaces. Mott-Schottky plots are most often used for electrochemistry on semiconductor electrodes. They can also be used to established type of semiconductivity of material and measure flat band potential and charge carrier density by following equation [3.6]

$$\frac{1}{C^2} = \frac{2}{N_d A^2 q \epsilon \epsilon_0} \left[ V - V_{fb} - \frac{kT}{q} \right] \quad (3.6)$$

Where C represents the space charge capacitance,  $N_d$  represents the charge carrier densities,  $q$  = electronic charge ( $1.602 \times 10^{-19}$  C),  $\epsilon$  = the dielectric constant of catalyst,  $\epsilon_0$  = the permittivity of free space ( $8.85 \times 10^{-12}$  F cm<sup>-2</sup>), V represents the applied potential,  $V_{fb}$  = flat band potential, k is the Boltzmann constant, and T is temperature in Kelvin scale. The term  $kT/q$ , being small, has been neglected. In the present study the Mott-Schottky analyses of catalysts were performed at a frequency of 10 kHz and applied potential 100 mV.

### 3.7.11 Brunauer–Emmett–Teller (BET) surface area

The surface area, pore size and pore volume of the catalysts were determined from N<sub>2</sub> adsorption/desorption technique using a Micromeritics (make USA) ASAP 2020 surface area and pore size analyser. The instrument had a provision to clean the sample by keeping the same in an evacuated chamber at elevated temperatures.

In the present study, the samples were evacuated to a pressure of  $1 \times 10^{-2}$  bar at 423 K for 2 h and subsequently at 623 K for 12 h. Samples along with the sample holder was then connected to the analysis port. The sample weight was kept in liquid nitrogen bath during the analysis. The dead space calibration was carried out using helium gas.



The amount of nitrogen gas adsorbed at any fixed desired pressure was recorded when equilibrium was reached. The data were recorded for pressure range ( $p/p^\circ$ ) from 0.001 to 0.995 where  $p^\circ$  is the vapor pressure of nitrogen. For adsorption studies the pressure was increased in increment till  $p/p^\circ = 0.995$  was reached. A total of 25 data were recorded. Once the final pressure was achieved desorption was carried out by decreasing pressure. For the surface area determination BET isotherm which account for multilayer physical adsorption was fitted for adsorption between  $p/p^\circ = 0.05$  and 0.35. Cross section area of nitrogen molecule was taken  $16.2 \text{ \AA}^2$ .